proceedings

MDPI

Proceedings

Assessment of Damage Distribution in Brittle Materials by Application of an Improved Algorithm for Three-Dimensional Localization of Acoustic Emission Sources with P-Wave Velocity Calculation †

Patricia Rodríguez [1,*] and Tarcisio B. Celestino [2,3,]

[1] Ferrara, Proyectos Especiales, Santiago 7770112, Chile
[2] Department of Geotechnical Engineering, São Carlos Engineering School, University of São Paulo, São Carlos, São Paulo 13566-590, Brazil; tbcelest@usp.br
[3] Themag Engenharia Ltd.a., São Paulo 01045-911, Brazil
* Correspondence: patricia.rodriguez@ferrara.cl or pcrodris@uc.cl; Tel.: +56-994-927-390
† Presented at the 18th International Conference on Experimental Mechanics (ICEM18), Brussels, Belgium, 1–5 July 2018.

Published: 18 June 2018

Abstract: The rupture process in brittle materials is associated with tensile stresses at microscopic flaw scale inside their volume. Acoustic emission monitoring of diametral compression tests is an adequate option to assess the progression of damage. An improved algorithm for AE sources localization with P-wave velocity, v_p, calculation and an enhanced methodology for P-wave onset time, called CLAPWaVe (Rodríguez 2015), is applied to analyze the distribution of damage and the evolution of stiffness within monzogranite specimens. Complementary analyses allowed the identification of four zones of damage accumulation within the specimen volume, each of them with different cracking levels, absolute energy release, E_A, associated v_p values, induced by different phenomena occurring during the loading process. The observed non-homogeneous damage distribution confirms that using a unique v_p value to perform the localization of all AE sources, as usually adopted, is not representative of the real condition of the specimen.

Keywords: three-dimensional localization of cracks; acoustic emission; damage distribution; v_p values evolution; CLAPWaVe

1. Introduction

Tensile stresses generated by local stress concentration at microscopic flaw scale inside quasi-brittle materials are responsible for the initiation and development of their rupture process. The crack propagation process releases energy as elastic waves, known as acoustic emission, AE [2]. Given the characteristics of the initiation of this damage process, experimental analyses of specimens subjected to tensile stresses monitored with AE is an adequate option to achieve a real understanding of this process.

The distribution of damage inside a specimen under loading can be obtained by three-dimensional localization of AE sources. Several works have reported on the three-dimensional localization of AE sources [2–7], but they consider v_p as a known value that remains unchanged while damage is induced in the specimen. This assumption is not realistic and may affect the accuracy of the localization process and the accuracy of the AE sources pattern obtained. Aker et al. [8] incorporated v_p calculation during the localization process but using a separate group of sensors specifically for this purpose. Li and Dong [9] proposed a solution for the three-dimensional

localization of AE sources with v_p calculation, but their algorithm requires previously known information about the onset of signal to each sensor. Since both the P-wave arrival time and the v_p value are dominant factors involved in the accuracy of the three-dimensional localization of AE sources, an algorithm incorporating improvements for both aspects, called CLAPWaVe (Crack Location by Acoustic emission with P-Wave Velocity determination) [1], is applied in this manuscript. CLAPWaVe is an iterative three-dimensional localization algorithm that includes a more efficient searching algorithm, an improved methodology for P-wave arrival time determination, independent of a predefined amplitude threshold, and calculates the coordinates of each AE source as well as the associated v_p value [1].

This manuscript reports on the application of CLAPWaVe to the characterization of the cracking process, the cracking pattern and evolution of integrity within a brittle material under diametral compression test. The characterization process is performed using complementary analyses of the pattern of localized AE sources and the distribution of both v_p and absolute energy release E_A inside the specimen volume during the loading process.

2. Materials and Methods

A total of 17 disc-shaped rock specimens with 100 mm diameter and 50 mm thickness were subjected to displacement-controlled diametral compression tests. The selected rock for this research was monzogranite, because of its brittle behavior and macroscopic homogeneity in its intact condition. The same concepts are applicable to other similar materials. A stiff servo-controlled testing system with maximum loading capacity of 2700 kN was used. The procedure suggested by Celestino et al. [10] was adopted to allow controlling the post-peak region of the test. An eight-channel system and six wide band piezoelectric AE sensors, developed by Physical Acoustics South America (PASA), were used to monitor the cracking process (three on each face of the rock specimens). A dual averaging extensometer was used to control the displacement along the diameter perpendicular to the loading direction. Figure 1 shows the typical test setup and instrumentation.

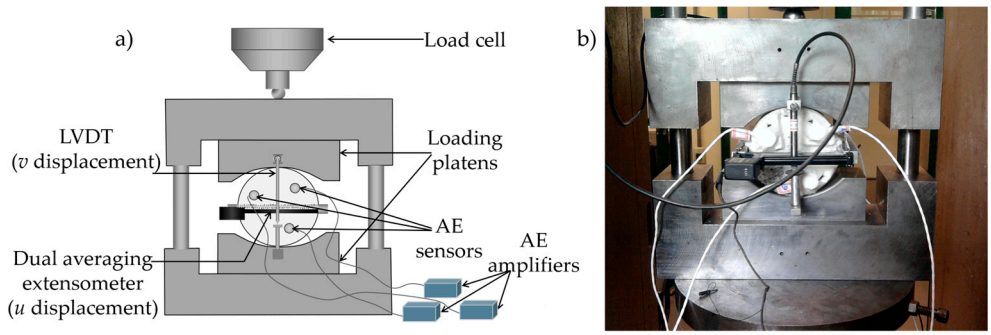

Figure 1. Schematic (**a**) and typical (**b**) test setup and instrumentation.

In order to analyze the cracking pattern and integrity of the specimen, the absolute energy E_A (aJ) of the signal is used. E_A is calculated as the integral of the square of the voltage $V(t)$ divided by the impedance of the AE system R [1] (t_d is the duration of the signal):

$$E_A = \frac{\int_0^{td} V(t)^2 \, dt}{R} \quad (1)$$

3. Results and Discussion

The localization algorithm of CLAPWaVe minimizes the error of searching for the coordinates of each AE source including v_p as another unknown variable in the iterative process. Thus, the v_p value associated to each AE source characterizes the mean properties of the specimen volume, defined along the trajectories between the AE source and each of the AE sensors that receive the signal emitted by this AE source. Therefore, the trend of the average v_p values associated to each AE

source allows the analysis of the distribution and evolution of damage, strength and stiffness inside the volume of the specimen during the loading process.

Figure 2 shows the spatial distribution of v_p values associated to each AE source during one test. Figure 2 displays seven control points, 1 to 7, representing loading stages at which variation of v_p inside of the specimen is presented (see load-time relationship at the bottom right of the figure). Control Points 1 to 3 are located at 50%, 75% and 100% of the peak load, respectively. Control Points 4 to 7 show different post peak stages of loading, including the end of the test. The different ranges of v_p values inside of the specimen are represented by a color scale, which is shown at the bottom left of the figure. The size of the dots shown in Images 1 to 3 of Figure 2 was increased to enable a better visualization of the pattern at the first loading stages, where only a few AE sources were localized. At the end of the test (Image 7), the large amount of AE sources localized might hinder a complete visualization of the pattern of v_p values in an XY plane. For the sake of clarity, a lateral view at the same stage (YZ plane) is shown at the middle right of the figure. In addition, a photograph of the final cracked specimen at the end of the test (Control Point 7) has been included at the bottom right of the figure.

Image 1 of Figure 2 shows only two AE sources localized at the region of contact between the specimen and the loading platens. Their location and the low levels of absolute energy released at this stage (see also Figure 3f) suggest that they are not related to the initiation of microcracking but to the process of adjustment between loading platens and specimen during initial loading stages.

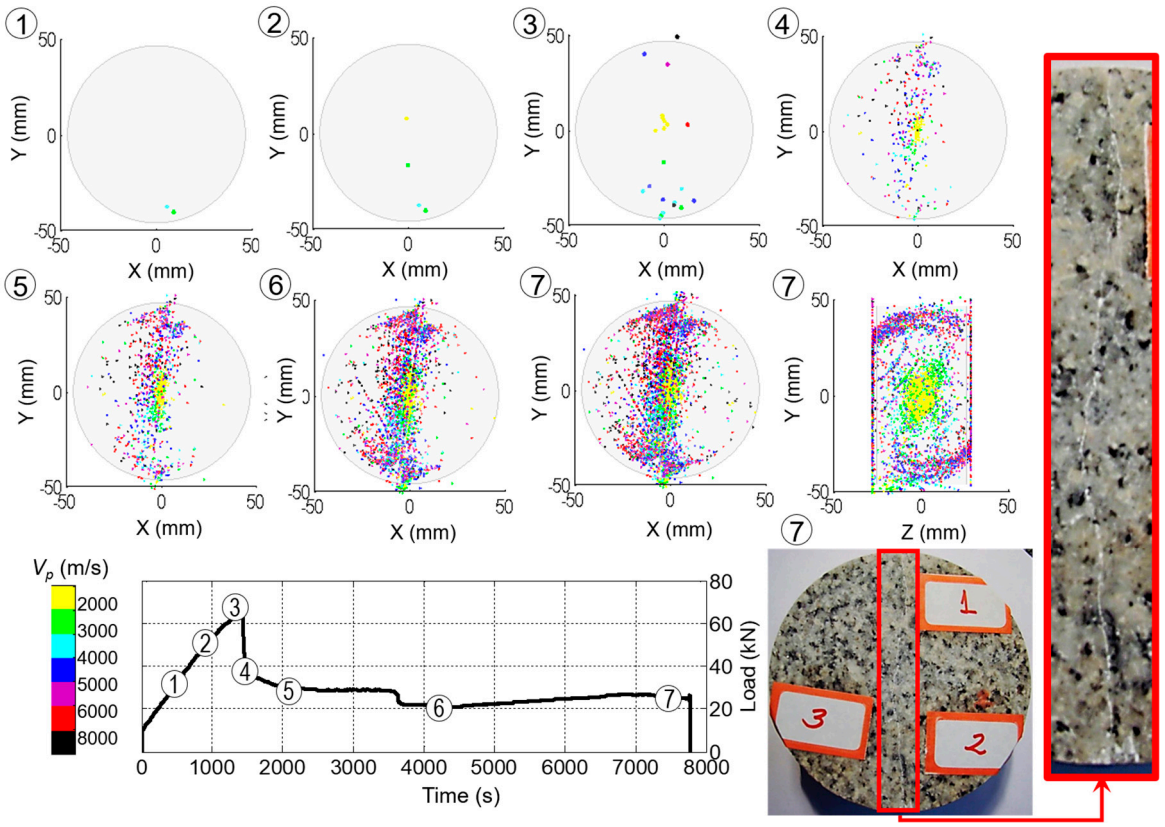

Figure 2. Typical distribution of average v_p values at different stages of loading during monotonic displacement diametral compression test on a monzogranite specimen. Photograph of the final cracking pattern on one of the faces of the specimen (**bottom left**) and magnified view of the cracked area in the red rectangle (**left**).

From control point 2 onwards, AE sources with v_p values lower than that of the intact condition (4659 m/s) accumulated at the center of the specimen. Their v_p values and the higher levels of E_A released (see Figure 2h) suggest they are associated with initiation and propagation of microcracking.

Images 2 to 7 of Figure 2 show that during the test a central damage core is generated. Such zone is composed by AE sources with v_p values much lower than that of the intact condition and lower than any other zone of the specimen. Images 7 (planes XY and YZ) show the clear damaged core zone, while the region of contact between the specimen and the loading platens show v_p values similar and even higher than that of the intact condition. Also, the region close to the faces of the specimen shows v_p values that oscillate around that of the intact condition. The pattern shown in Images 7 of Figure 2 is in good agreement with the general cracking pattern of the real rock specimen (bottom right of Figure 2).

By performing complementary analyses of the v_p values, the pattern of AE sources and the accumulated E_A of each AE source, four zones of damage accumulation with different characteristic were identified: contact region (blue sources, Figure 3a), internal core (red sources, Figure 3b), external core (green sources, Figure 3c), boundary zone (pink sources, Figure 3d). The contact zone contains the AE sources located close to the region of contact between the specimen and the loading platens; the internal core contains the AE sources located in a close vicinity of the center of the specimen; and the external core contains those located in the central region of the specimen, but close to its faces. Those three zones are located along the loading axis, defining the typical failure surface observed in diametral compression tests (see photograph at the bottom right of Figure 2).

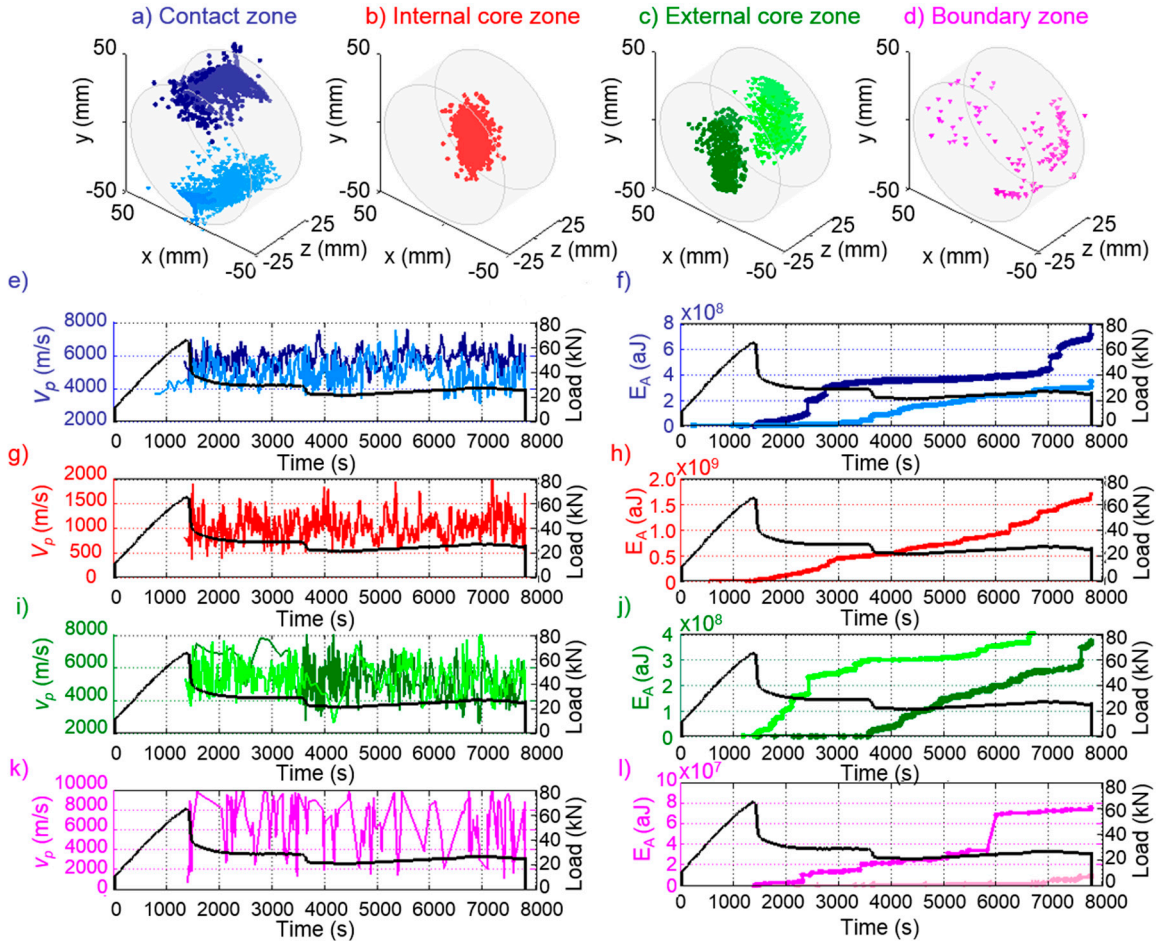

Figure 3. Distribution of damage obtained by application of CLAPWaVe to a monzogranite specimen under diametral compression test. Identified zones of damage (**a**–**d**) and distribution of v_p and E_A for contact zone (**e**,**f**), central core (**g**,**h**), external core (**i**,**j**) and boundary zone (**k**,**l**).

The v_p values are calculated for each AE source localized by means of a process that involves the minimization of the adjustment error. In addition, each v_p value is associated with a region in the specimen volume limited by the AE source and by the sensors taken to localize it. The integrity of such region changes with the loading process. Therefore, v_p values change along the process, even for data coming from the same zone. For that reason, analyses of v_p values representative of the different zones at different loading stages shown in Figure 3e,g,i,k are performed considering the trend of a moving average and not every single value.

Figure 3e shows that AE sources are first localized at the contact zone (at the bottom part of the specimen for this test, but in other tests it initiates at the top). The values of v_p associated with the first AE sources are close to that of intact material, but as the load increases, v_p also increases, showing the effect of confinement induced by the loading platens in the specimen. Theoretical expressions [11,12] as well as numerical simulations [13], both performed considering specimens of homogeneous material subjected to diametral compression, showed that stresses on the X-axis are compressive close to the region of contact between the specimen and the loading platens. Also, in diametral compression tests, when a compressive load is applied along the Y-axis of the specimen, the higher stiffness and Poisson's ratio of the loading platens in comparison with those of the rock specimen induce compressive stresses along the Z-axis in the region of contact. Therefore, a three-dimensional confinement effect develops in that region, which increases with loading. The confinement increases the stiffness of the specimen in this zone, producing v_p values similar to or even higher than those of the intact specimen condition. As the load increases, so does the damage in this contact zone (See Figure 3e,f), therefore, the v_p value stabilizes instead of increasing through the end of the test.

Figure 3g,h suggest the generation of a damaged central core, with the lowest v_p values of the specimen (much lower than that of the intact condition) and the highest levels of E_A release. As expected for this type of test, the central core zone shows the main concentration of damage (approximately 55% of the AE sources localized throughout the test) and the highest stiffness decrease.

In the external core zone (Figure 3i), the associated v_p values oscillate around the v_p of the specimen in the intact condition, even though microcracking progresses in this zone (high levels of E_A in Figure 3j). This behavior is explained by considering that the waves generated in the external core zone have to travel through highly damaged zones and other almost undamaged zones to reach the sensors.

The natural microscopic heterogeneity of the specimens explains the slightly asymmetrical distribution of damage on the faces of the specimen (E_A in Figure 3f) and at its top and bottom (E_A in Figure 3j).

The boundary zone (Figure 3d) is a region with secondary microscopic cracking, generated as a result of the main damaging process developed through the failure surface. After the failure surface has been created following the loading axis of the specimen, the bending of its two halves may induce tension at the external borders, outside the center of the specimen. Figure 3d shows scarce AE sources localized in this boundary zone (less than 2% of the total of AE sources localized during the entire test). Secondary microcracking is consistent with the existence of AE sources in this zone only at later stages of the test (after damage has progressed through the other three zones); and with the low level of EA associated to them (100 times lower than those of the internal core and 10 times lower than those of the external core or contact region). The low number of AE sources in this zone and the strong influence of the other three zones on the trajectory of waves from the source to the sensors does not allow the visualization of a clear pattern of v_p values.

4. Conclusions

An improved algorithm for AE sources localization with v_p calculation and an enhanced methodology for the P-wave onset time, called CLAPWaVe, is applied here to assess the distribution of damage and evolution of stiffness within monzogranite specimens subjected to diametral compression tests.

The determination of the average v_p values associated with each AE source localized provided important information related to the distribution and evolution of damage and stiffness variability within the volume of the specimens as well as during the loading process. Complementary analyses of the pattern of AE sources and their associated v_p values and EA showed a non-homogeneous distribution of damage, changing the characteristics of the specimen in comparison with its initial intact condition. Therefore, the use of a unique value for v_p equal to that of the intact condition to localize all AE sources throughout the test is not representative of the real condition of the specimen and may lead to unrealistic analyses.

Further research is still needed to determine the main reasons for the large variation of P-wave velocity observed. The possible causes are: (i) nonlinearity of the wave propagation process leading to dependence of v_p on the E_A level; (ii) velocity tends to be lower in a zone subjected to tensile stresses due to microcrack opening, and higher in compressed zones; (iii) once a crack opens in a tensioned zone, tensile stresses are released, and the velocity increases again.

Author Contributions: This work is the partial result of the doctoral research of the first author, P.R., at the University of São Paulo, Brazil. The second author, Tarcisio B. Celestino was the research supervisor. T.B.C. conceived the idea of three-dimensional localization with P-wave calculation. P.R. performed the experiments and developed the CLAPWaVe. Both authors analyzed the data and wrote the paper.

Acknowledgments: Financial support for the acquisition of the acoustic emission equipment was provided by FAPESP, the research funding agency for the State of São Paulo, Brazil (process No. 05/57250-2). The scholarship for the doctoral research of the first author was provided by CONICYT, the national research council of Chile (document No. 72120096).

Conflicts of Interest: The authors declare no conflict of interest. The founding sponsors had no role in the design of the study; in the collection, analyses, or interpretation of data; in the writing of the manuscript, and in the decision to publish the results.

References

1. Rodríguez, P. Analysis of Microcracking in Rocks in Diametral Compression Tests. Ph.D. Thesis. University of São Paulo, São Carlos, Brazil, 2015.
2. Labuz, J.F.; Cattaneo, S.; Chen, L.H., Acoustic emission at failure in quasi-brittle materials. *Constr. Build. Mater*. **2001**, *15*, 225–233, doi:10.1016/S0950-0618(00)00072-6.
3. Iverson, N.; Kao, C.; Labuz, J.F. Clustering analysis of AE in rock. *J. Acoust. Emiss*. **2007**, *25*, 364–372.
4. Jian-po, L.; Yuan-hui, L.; Shi-da, X.; Shuai, X.; Chang-yu, J. Cracking mechanisms in granite rocks subjected to uniaxial compression by moment tensor analysis of acoustic emission. *Theor. Appl. Fract. Mech.* **2015**, *75*, 151–159, doi:10.1016/j.tafmec.2014.12.006.
5. Han, Q.; Xu, J.; Carpinteri, A.; Lacidogna, G. Localization of acoustic emission sources in structural health monitoring of masonry bridge. *Struct. Control Health Monitor.* **2015**, *22*, 314–329, doi:10.1002/stc.1675.
6. Rodríguez, P.; Arab, P.; Celestino, T.B. Characterization of rock cracking patterns in diametral compression tests by acoustic emission and petrographic analysis *Int. J. Rock Mech. Min. Sci*. **2016**, *83*, 73–85, doi:10.1016/j.ijrmms.2015.12.017.
7. Ciampa, F.; Meo, M. A New algorithm for acoustic emission localization and flexural group velocity. *Compos. Part A Appl. Sci. Manuf.* **2010**, *41*, 1777–1786, doi:10.1016/j.compositesa.2010.08.013.
8. Aker, E.; Kühn, D.; Vavryčuk, V.; Soldal, M.; Oye, V. Experimental investigation of acoustic emissions and their moment tensors in rock during failure. *Int. J. Rock Mech. Min. Sci.* **2014**, *70*, 286–295, doi:10.1016/j.ijrmms.2014.05.003.
9. Li, X.; Dong, L. An Efficient closed-form solution for acoustic emission source location in three-dimensional structures. *AIP Adv.* **2014**, *4*, 027110, doi:10.1063/1.4866170.
10. Celestino, T.; Bortolucci, A.; Nobrega, C. Determination of rock fracture toughness under creep and fatigue. In *Proceedings of the US Symposium on Rock Mechanics*; CRC Press: Boca Raton, FL, USA, 1995; pp. 147–152.
11. Chau, K.T.; Wei, X.X. A Three-dimensional analytic solution for the brazilian test. In Proceedings of the 2nd Asian Rock Mechanics Symposium, Beijing, China, 11–14 September 2001; pp. 141–144.

12. Hondros, G. The Evaluation of poisson's ratio and the modulus of materials of a low tensile resistance by the Brazilian (indirect tensile) test with particular reference to concrete. *Aust. J. Appl. Sci.* **1959**, *10*, 243–268.
13. Li, D.; Wong, L.N.Y. The brazilian disc test for rock mechanics applications: Review and new insights. *Rock Mech. Rock Eng*. **2013**, 269–287, doi:10.1007/s00603-012-0257-7.